Journal of Sound and Vibration (2000) **237**(3), 411–426
doi:10.1006/jsvi.2000.3041, available online at http://www.idealibrary.com on IDEAL®

STRUCTURAL MODIFICATION BASED ON MEASURED FREQUENCY RESPONSE FUNCTIONS: AN EXACT EIGENPROPERTIES REALLOCATION

Y.-H. PARK AND Y.-S. PARK*

Department of Mechanical Engineering, Center for Noise and Vibration Control, Korea Advanced Institute of Science and Technology, Science Town, Taejon 305-701, *Korea. E-mail*: *yspark@mail.kaist.ac.kr*

(*Received* 13 *October* 1999, *and in final form* 14 *April* 2000)

A structural modification method based on frequency response functions is presented in terms of an inverse eigenvalue problem. The design objective is to derive multiple lumped mass, damper and stiffness modifications needed to reallocate eigenvalues and specify eigenvectors of an existing structure. A frequency response function-based substructure-coupling concept is used to get the system dynamic equations. A linear algebraic equation is finally obtained to identify the necessary structural modifications. The exact structural modifications are determined. The existence and uniqueness of exact solutions are also investigated. The feasibility of structural modification is examined under the restrictions of structural modifications in the case where infinite many exact modifications can exist. The proposed method was applied to an example structure. Based on experiment data, the minimum stiffness modifications were calculated. The result of application indicates that the suggested method can derive accurate structural changes just based on minimum number of measured frequency response functions.

1. INTRODUCTION

Structural modifications are often undertaken to improve the dynamic behavior of an existing structure. In many cases, the objective is to modify structure eigenvalues or eigenvectors to reduce the vibration responses of the structure. There are two opposite approaches for structural modifications. The first one is a forward problem, in which new modified eigenproperties are predicted utilizing the structural changes together with the original modal properties. The second one is questioning about the necessary structural modifications which satisfy the desired eigenproperties. This one is an inverse problem and its solution can be non-unique or non-existent depending on the target modes and the given restrictions on the structural modifications. This paper deals with this inverse problem accounting especially the local modifications, i.e., lumped mass, stiffness and damping modifications. Special interest is given in this paper to utilizing only the experimental data obtained from the existing structure throughout the solution procedure.

Many approaches have been suggested to solve this inverse problem based on modal information. Modal perturbation [1] and localized modification methods [2, 3] were introduced to change structure eigenvalues. Some researchers utilized iterative method combined with eigenvalues sensitivity [4]. But these modal domain methods provide the

*Author to whom correspondence should be addressed.

0022-460X/00/430411 + 16 $35.00/0

accurate solutions of the inverse problem as long as the amount of structural modification is small or that is just a simple rank-one (i.e., single lumped mass or linear stiffness) modification [5]. The major reason for this limitation is due to the so-called modal truncation error [6, 7]. In most cases, the truncated modal model is obtained from both of the FE analysis and the experimental modal analysis since only a subset containing lower modes are available in numerical calculation and in test as well. Up to recent years, alternative methods have been introduced to find the exact solutions of the inverse problem by relieving this modal truncation error. Bucher and Braun assumed the desired new mode shape to be a linear combinations of unmodified modal vectors [8]. Tsuei [9, 10], Li [11] and Park [12] addressed frequency response function (FRF) formulations to relocate modal frequencies.

Thus, this paper endeavors to find analytically the necessary multiple mass, stiffness and damping modifications in order to exactly achieve both of required eigenvalues and eigenvectors. The test-based FRF of unmodified structure is used throughout this solution procedure.

For the theory development, a substructure-coupling concept is introduced. Frequency response functions of the original structure and those of adding substructures are coupled at the connecting degrees of freedom (d.o.f.) by using force equilibrium and geometric compatibility constraints. Finally, a linear algebraic identification equation is obtained to solve the inverse eigenvalue problem. No iteration is needed for obtaining the exact solution of the inverse problem but it can be determined analytically by solving this linear algebraic equation. The existence and uniqueness of the exact solutions are investigated. A special attention is given to the case where infinite many structural modifications are possible, in which the least modification can be determined among the possible modifications. The proposed method is applied to a plate structure which is redesigned to have a specified natural frequency and nodal point. The resulting modifications were checked by experiment and their effectiveness was discussed.

2. PROBLEM DEFINITION

The problem definition of this paper is how to add multiple lumped masses, linear grounded stiffnesses and dampers to a baseline structure in order to change the system natural frequency to a desired value ω_n and also to specify the modeshape to a desired modal vector ϕ_n. In this problem, each added structure is assumed to be either mass–damper system or stiffness–damper system. Figure 1 shows the schematic diagram for

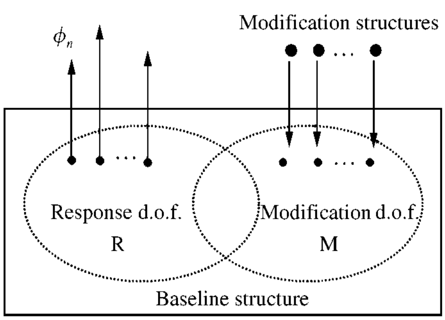

Figure 1. Multiple lumped structural modifications at designated modification d.o.f. in domain M and modeshape ϕ_n defined in domain R for a natural frequency ω_n.

the suggesting problem. The modification d.o.f. are designated to N_M specified locations in domain M and a mass–damper system or a stiffness–damper system can be added to each point. The desired modal vector ϕ_n is defined on partially selected N_R locations in domain R. The desired eigenproperties, i.e., ω_n and ϕ_n, can be assigned arbitrarily.

3. FREE VIBRATION EQUATIONS

This modified structure can be divided into several substructures. Thus, baseline structure and modification structures are coupled at the interface d.o.f. in domain M as shown in Figure 1. Each modification substructure is connected to baseline structure at each interface node. For free vibration case, no external force is exerted on the substructures except the internal forces at the interfaces. The equation of motion of the substructures can be described in the stacked form as

$$\begin{bmatrix} \mathbf{H}^b_{MM}(\omega_n) & \mathbf{0} \\ \mathbf{0} & \mathbf{H}^m_{MM}(\omega_n) \end{bmatrix} \begin{bmatrix} \mathbf{f}^b_M \\ \mathbf{f}^m_M \end{bmatrix} = \begin{bmatrix} \mathbf{x}^b_M \\ \mathbf{x}^m_M \end{bmatrix}, \tag{1}$$

where the superscripts b and m denote baseline structure and modification structures, respectively, and the subscript M denotes modification d.o.f. $\mathbf{H}^b_{MM}(\omega)$ and $\mathbf{H}^m_{MM}(\omega)$ are the frequency response function (FRF) matrices of substructures containing the FRFs between the interface d.o.f. in domain M. $\mathbf{f}^b_M$ and $\mathbf{f}^m_M$ are the internal force vectors acting on substructures and $\mathbf{x}^b_M$, $\mathbf{x}^m_M$ are the displacement vectors defined in domain M. The forces and the displacements in equation (1) are subject to the force equilibrium and the geometric compatibility constraints as follows:

$$\mathbf{f}^b_M + \mathbf{f}^m_M = \mathbf{0}, \tag{2}$$

$$\mathbf{x}^b_M = \mathbf{x}^m_M. \tag{3}$$

Due to the constraints in equations (2) and (3), not all of the forces and displacements in equation (1) are independent. By substituting equations (2) and (3) into equation (1) and rearrange it with respect to $\mathbf{f}^b_M$, we have the free vibration equation of combined structure for the independent force vector $\mathbf{f}^b_M$ as

$$[\mathbf{H}^b_{MM}(\omega_n) + \mathbf{H}^n_{MM}(\omega_n)]\mathbf{f}^b_M = \mathbf{H}(\omega_n)\,\mathbf{f} = \mathbf{0}. \tag{4}$$

Equation (4) is called the modal force equation [9, 12], which is a key equation in this study. Non-trivial solution of $\mathbf{f}^b_M$ is denoted by the modal force vector $\mathbf{f}$, which consists of the internal forces acting on the baseline structure when the combined structure vibrates freely. The modal force matrix, $\mathbf{H}(\omega_n)$ is the summation of FRF matrix of the baseline structure, $\mathbf{H}^b_{MM}(\omega_n)$ and that of the modification substructures, $\mathbf{H}^m_{MM}(\omega_n)$. Considering the modification structures composed of lumped mass–damper systems and stiffness–damper systems, the matrix $\mathbf{H}^m_{MM}(\omega_n)$ in equation (4) can be written in detail as

$$\mathbf{H}^m_{MM}(\omega_n) = \begin{bmatrix} h_1(\omega_n) & 0 & 0 & 0 \\ 0 & h_2(\omega_n) & 0 & 0 \\ 0 & 0 & \ddots & \vdots \\ 0 & 0 & \cdots & h_{N_M}(\omega_n) \end{bmatrix}. \tag{5}$$

$h_j(\omega_n)$ in equation (5) is the point receptance of the jth modification substructure at the natural frequency ω_n and it is simply

$$h_j(\omega_n) = \frac{1}{d_j(\omega_n)} = \frac{1}{-\omega_n^2 m_j + \mathrm{i}\omega_n c_j} \quad \text{for mass–damper modification} \tag{6}$$

or

$$h_j(\omega_n) = \frac{1}{d_j(\omega_n)} = \frac{1}{k_j + \mathrm{i}\omega_n c_j} \quad \text{for stiffness–damper modification} \tag{7}$$

where $d_j(\omega_n)$ denotes dynamic stiffness of the jth modification substructure, and m_j, c_j and k_j (for $j = 1, 2, \dots, N_M$) are the amounts of mass, damper and stiffness modifications, respectively, which are positive definite. Experimentally measured FRFs of the baseline structure can be used directly to form the modal force equation bypassing the numerical modelling process as shown in equation (4).

The assigned modeshape ϕ_n is obviously the frequency response due to modal force $\mathbf{f}$ at this desired natural frequency such that

$$\phi_n = \mathbf{H}^b_{RM}(\omega_n)\mathbf{f}, \tag{8}$$

where $\mathbf{H}^b_{RM}(\omega_n)$ is the cross FRF matrix between d.o.f. in domain R and those in domain M shown in Figure 1.

Note that equations (4) and (8) are the necessary and sufficient conditions for the requirements that ω_n becomes a new system natural frequency and ϕ_n is corresponding mode shape. Hence, the FRFs of the modification substructures in equation (5) are the exact solution for the given eigenproperty assignment when equations (4) and (8) are satisfied simultaneously.

4. DETERMINATION OF EXACT STRUCTURAL MODIFICATIONS

The solution procedure for finding structural parameters starts from the force–response relation in equation (8). Modal force vector $\mathbf{f}$ can be identified from equation (8) if $N_M = N_R$ and $\mathbf{H}^b_{RM}(\omega_n)$ is invertible as

$$\mathbf{f} = \mathbf{H}^b_{RM}(\omega_n)^{-1}\phi_n. \tag{9}$$

By substituting equation (5) into equation (4), we can have a linear algebraic equation for the FRFs of modification substructures, i.e., $h_j(\omega_n)$ for $j = 1, 2, \dots, N_M$ as

$$\begin{bmatrix} f_1 & 0 & 0 & 0 \\ 0 & f_2 & 0 & 0 \\ 0 & 0 & \ddots & \vdots \\ 0 & 0 & \cdots & f_{N_M} \end{bmatrix} \begin{bmatrix} h_1(\omega_n) \\ h_2(\omega_n) \\ \vdots \\ h_{N_M}(\omega_n) \end{bmatrix} = -\mathbf{H}^b_{MM}(\omega_n)\mathbf{f}, \tag{10}$$

where f_j is the jth modal force in $\mathbf{f}$ which is identified by equation (9). By solving this algebraic equation, $h_j(\omega_n)$ can be obtained as

$$h_j(\omega_n) = \frac{1}{d_j(\omega_n)} = -\frac{\lfloor \mathbf{H}^b_{MM}(\omega_n) \rfloor_j^{\mathrm{T}} \mathbf{f}}{f_j} \quad \text{for } j = 1, 2, \dots, N_M, \tag{11}$$

where $\lfloor \mathbf{H}^b_{MM}(\omega_n) \rfloor_j$ is the jth row vector of $\mathbf{H}^b_{MM}(\omega_n)$.

The necessary structural parameters at the jth modification point can be determined straightforwardly by substituting calculated $h_j(\omega_n)$ in equation (11) into equation (6) or equation (7) as follows. By comparing the real parts of equations (6) and (7), mass m_j or stiffness k_j can be determined according to the signs of the real parts since m_j and k_j are positive definite as follows:

$$m_j = -\frac{1}{\omega_n^2}\mathrm{Re}\,[d_j(\omega_n)] \quad \text{when Re}\,[d_j(\omega_n)] < 0 \tag{12}$$

or

$$k_j = \mathrm{Re}\,[d_j(\omega_n)] \quad \text{when Re}\,[d_j(\omega_n)] > 0 \tag{13}$$

for $j = 1, 2, \ldots, N_M$. Negative real part of the jth dynamic stiffness means that the mass effect is required at the jth location for achieving the given eigenproperties, and its positive real part means that the stiffening effect is required at the same location. Mass and stiffness in equations (12) and (13) are the realizations of the necessary physical effects of the modifications on the baseline structure. By comparing the imaginary parts of equations (6) and (7), the damping parameter c_j can be determined. Since c_j is positive definite, it is

$$c_j = \frac{1}{\omega_n}\mathrm{Im}\,[d_j(\omega_n)] \quad \text{when Im}\,[d_j(\omega_n)] > 0. \tag{14}$$

Positive imaginary part of the jth dynamic stiffness implies that energy dissipation is needed at the jth location in order to meet the given eigenproperty change and it can be realized with the passive damping element as shown in equation (14). However, if the jth dynamic stiffness has negative imaginary part then the damping parameter should be negative, which cannot be realized by the passive damping element. It means that in this case an energy source element, e.g., an excitation device, is required at that node for achieving the given eigen properties.

When singular condition occurs in equation (11), i.e., $f_j = 0$, in other words if no internal force is required at the jth node, any kind of structural element need not be added at that position. For the condition that $h_j(\omega_n) = 0$ in equation (11), i.e., dynamic stiffness goes to infinity, we know that the jth node should be rigidly supported obviously. The structural modifications determined in equations (12)–(14) are the exact solutions for achieving the given eigenstructure under the assumptions that the measured FRFs are free of noise. Any arbitrary natural frequencies and modal vectors of size N_R except those requiring energy source elements can be achieved by adding the multiple mass–damper systems and stiffness–damper systems described in equations (12)–(14). But due to the practical limitations of hardware, not all of the structural modifications can be realizable although exact solutions are known in principle.

5. EXISTENCE AND UNIQUENESS OF EXACT SOLUTION

A unique set of exact structural modifications can be determined straightforwardly for an identified modal force vector as described in section 4. Hence, the number of exact solution is equal to the number of modal force vectors which satisfy the mode shape requirement shown in equation (8). Considering equation (8), it can be stated about the existence and uniqueness of the exact structural modifications for a given eigenproperty requirement as follows:

Case 1. *A unique set of exact structural modification exists* when $N_M = N_R$ and $\mathbf{H}^b_{RM}(\omega_n)$ is invertible. In this case, the modal force vector is

$$\mathbf{f} = \mathbf{H}^b_{RM}(\omega_n)^{-1}\phi_n. \tag{15}$$

Case 2. *Infinite many sets of exact structural modifications exist* when $N_M > N_R$. In this case, the modal force vector is underdetermined [13] as

$$\mathbf{f} = \mathbf{f}^0 + \sum_{i=1}^{N_M - N_R} c_i \mathbf{f}^i, \tag{16}$$

where $\mathbf{f}^0 = \mathbf{H}^b_{RM}(\omega_n)^+ \phi_n$ and superscript + denotes the pseudo-inverse matrix, $c_1, c_2, \ldots, c_s$ ($s = N_M - N_R$) are arbitrary redundant parameters and $\mathbf{f}^i$ is the ith null vector of $\mathbf{H}^b_{RM}(\omega_n)$, i.e., $\mathbf{f}^i$ satisfies

$$\mathbf{H}^b_{RM}(\omega_n)\mathbf{f}^i = 0 \quad \text{for } i = 1, 2, \ldots, N_M - N_R. \tag{17}$$

For a special case when $N_M = 1$ and $N_R = 0$, i.e., single structural modification without modeshape constraint, the solution is unique since the scalar underdetermined modal force in both sides of equation (10) can be cancelled out and it does not affect the solution.

Case 3. *Exact structural modification does not exist* when $N_M < N_R$. In this case, the modal force vector is overdetermined. The least-squares error solution of modal force vector is

$$\mathbf{f} = \mathbf{H}^b_{RM}(\omega_n)^+ \phi_n. \tag{18}$$

For a special case when the given mode shape vector is included in the range space of $\mathbf{H}^b_{RM}(\omega_n)$, exact structural modification exists [13].

6. DETERMINATION OF MODIFICATION AMONG INFINITE MANY SOLUTIONS FOR UNDAMPED STRUCTURES

In previous sections, the exact solutions of inverse eigenvalue problem were considered. However, although the solutions described in equations (12)–(14) are exact in principle, actually achievable structural modifications can be restricted. In the practical point of view, the structural modifications at some limited number of positions are applicable. Sometimes the amount of mass and stiffness modifications should be limited also. Then the minimum modification among the feasible solutions can be preferred. In some practical structures operating in free–free boundary condition, e.g., aircraft and rockets, the ground stiffness modification cannot be achievable but the mass modifications are feasible. In this section, a procedure to determine the structural modifications under their restrictions mentioned above is presented.

As shown in section 5, infinite many structural modifications which achieve the given eigenproperties exist when modal force vectors are underdetermined. Considering the hardware restrictions on the structural modifications, how to select the best one among those infinite many solutions may be a question at this moment. In this section, an approximate but simplified procedure for selecting the best modification will be described under the assumption that the baseline structure is undamped. Under this assumption, the FRFs of the baseline structure can be assumed to be real-valued functions and consequently the structural modifications are restricted to the mass and stiffness additions as one can see in equations (12) and (13).

By substituting equation (16) into equation (11), the dynamic stiffness of the jth adding structural element can be written in terms of redundant parameters ($c_1, c_2, \ldots, c_s$) as

$$d_j(\omega_n) = \frac{f_j}{-\lfloor \mathbf{H}^b_{MM}(\omega_n) \rfloor^{\mathrm{T}}_j \mathbf{f}} = \frac{f_j^0 + \sum_{i=1}^s c_i f_j^i}{g_j^0 + \sum_{i=1}^s c_i g_j^i} \equiv \frac{f_j(\mathbf{c})}{g_j(\mathbf{c})}, \tag{19}$$

where $\mathbf{c} = [c_1, c_2, \ldots, c_s]^{\mathrm{T}}, f_j^i = \lfloor \mathbf{f}^i \rfloor_j$ and $g_j^i = -\lfloor \mathbf{H}^b_{MM}(\omega_n) \rfloor^{\mathrm{T}}_j \mathbf{f}^i$ (for $i = 0, 1, 2, \ldots, s$ and $j = 1, 2, \ldots, N_M$). When the baseline structure is undamped and normal mode shape ϕ_n is considered, all of functions and variables in equation (19) are real-valued. The sign of $d_j(\omega_n)$ in equation (19), which varies with the parameters ($c_1, c_2, \ldots, c_s$), determines which kind of structural modification among mass and stiffness is applicable as shown in equations (12) and (13). Thus, the structural modification at the jth node (for $j = 1, 2, \ldots, N_M$) can be determined directly by examining the signs of $f_j(\mathbf{c})$ and $g_j(\mathbf{c})$ as follows:

mass modification is feasible when $f_j(\mathbf{c}) \cdot g_j(\mathbf{c}) < 0$, (20)

stiffness modification is feasible when $f_j(\mathbf{c}) \cdot g_j(\mathbf{c}) > 0$, (21)

need not to be modified when $f_j(\mathbf{c}) = 0$, (22)

rigid support is feasible when $g_j(\mathbf{c}) = 0$. (23)

The restrictions on the amount of mass or stiffness modification at the jth node can be described by the following inequalities:

$$m_j \leqslant \mathrm{M}_{max}, \tag{24}$$

$$k_j \leqslant \mathrm{K}_{max}, \tag{25}$$

where M_{max} and K_{max} are the maximum allowed mass and stiffness modifications. Equations (24) and (25) also can be written in terms of redundant parameters ($c_1, c_2, \ldots, c_s$) using equations (12), (13) and (19) as follows:

$$\text{for mass constraints} \quad r_{mj}(\mathbf{c}) = r_{mj}^0 + \sum_{i=1}^s c_i r_{mj}^i \begin{cases} \geqslant 0 & \text{when } g_j(\mathbf{c}) > 0, \\ \leqslant 0 & \text{when } g_j(\mathbf{c}) < 0, \end{cases} \tag{26}$$

$$\text{for stiffness constraints} \quad r_{kj}(\mathbf{c}) = r_{kj}^0 + \sum_{i=1}^s c_i r_{kj}^i \begin{cases} \geqslant 0 & \text{when } g_J(\mathbf{c}) > 0, \\ \leqslant 0 & \text{when } g_j(\mathbf{c}) < 0, \end{cases} \tag{27}$$

where $r_{mj}^i = f_j^i + \omega_n^2 \mathrm{M}_{max} g_j^i$ and $r_{kj}^i = -f_j^i + \mathrm{K}_{max} g_j^i$ for $i = 0, 1, 2, \ldots, s$ and $j = 1, 2,, \ldots, N_M$. To get the practically achievable structural modification at the jth node, the redundant parameters ($c_1, c_2, \ldots, c_s$) should be selected to satisfy one of the equations (20)–(23), and also satisfy equation (26) or equation (27).

The constraints in equations (20)–(23) and equations (26) and (27) can be examined systematically by using the following vector space approach. Consider the hyperplanes, which are defined in a s-dimensional linear spaces as

$$f_i(\mathbf{c}) = f_j^0 + \sum_{i=1}^s c_i f_j^i = 0, \tag{28}$$

$$g_j(\mathbf{c}) = g_j^0 + \sum_{i=1}^s c_i g_j^i = 0, \tag{29}$$

where $\mathbf{c} = [c_1, \ c_2, \dots , c_s]^{\mathrm{T}}$ denotes a state vector which represents the point in an s-dimensional linear space. The normal vectors of those planes are

$$\mathbf{n}_{fj} = [f_j^1, f_j^2, \dots , f_j^s]^{\mathrm{T}} \quad \text{for } f_j(\mathbf{c}) = 0, \tag{30}$$

$$\mathbf{n}_{gj} = [g_j^1, \ g_j^2, \dots , g_j^s]^{\mathrm{T}} \quad \text{for } g_j(\mathbf{c}) = 0. \tag{31}$$

The hyperplane $f_j(\mathbf{c}) = 0$ divides the s-dimensional linear space into two half-spaces and so does the hyperplane $g_j(\mathbf{c}) = 0$. $f_j(\mathbf{c})$ and $g_j(\mathbf{c})$ have positive values when the point $\mathbf{c}$ is placed in the upper half-spaces of those hyperplanes, i.e., the half-spaces in normal vector directions from the hyperplanes. The signs of $f_j(\mathbf{c})$ and $g_j(\mathbf{c})$ alter when the point $\mathbf{c}$ crosses over those hyperplanes. The signs of $r_{mj}(\mathbf{c})$ and $r_{kj}(\mathbf{c})$ can be examined by using their hyperplanes $r_{mj}(\mathbf{c}) = 0$ and $r_{kj}(\mathbf{c}) = 0$ as references in the similar way. For an illustration, a structural modification problem involving three modification nodes ($N_M = 3$) and one modeshape constraint ($N_R = 1$) is considered. In this case, the modal force vector defined in equation (8) is underdetermined and has two redundant parameters, i.e., $\mathbf{c} = [c_1, c_2]^{\mathrm{T}}$. Thus, hyperplanes in equations (28) and (29) for the first node ($j = 1$) form lines in c_1–c_2 plane as shown in Figure 2. Those two lines divide c_1–c_2 plane into four sub-regions, which can be matched to the corresponding structural modifications determined from equations (20) and (21). Redundant parameters (c_1, c_2) on the line $g_1(\mathbf{c}) = 0$ yield rigid support and those placed on $f_1(\mathbf{c}) = 0$ yield no modification at the first node for achieving the given eigenproperties according to equations (22) and (23). Assuming that mass modification is desired for the first node, then the redundant parameters (c_1, c_2) should be selected in region A or region B. If the mass is limited as equation (24), then the feasible region of (c_1, c_2) shrinks to region B_1 since the constraint in equation (26) as well as equation (20) should be satisfied. Obviously, the mass modification under its constraint in equation (26) is shown to be feasible for achieving the given eigenproperties because the region B_1 is not empty. Two other structural modifications for the rest of nodes M_2 and M_3 can be examined by the same way.

In general case, when s redundant parameters are involved, the hyperplanes $f_j(\mathbf{c}) = 0$, $g_j(\mathbf{c}) = 0$, $r_{mj}(\mathbf{c}) = 0$ and/or $r_{kj}(\mathbf{c}) = 0$ (for $j = 1, 2, \dots , N_M$) can be expressed explicitly in terms of the linear equations of redundant parameters $(c_1, \ c_2, \dots , c_s)$. Using these hyperplanes the feasibility of trial structural modifications can be examined analytically

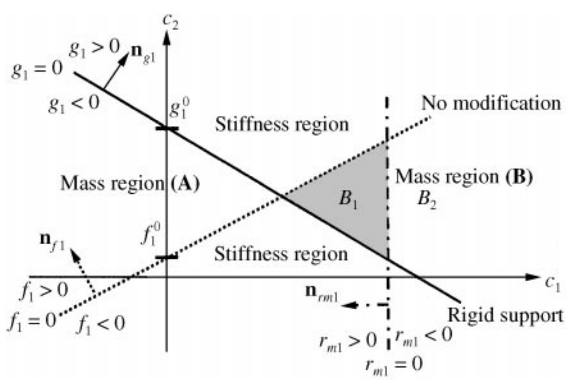

Figure 2. Redundant parameters (c_1, c_2) and corresponding feasible structural modifications for the first node ($j = 1$); regions A and B are feasible for mass modification and region B_1 is feasible for mass modification together with its constraint in equation (24).

through the same vector space approach described in the above illustration. Though the hyperplanes are known in explicit forms, somehow complicated calculations are required to identify the sub-regions surrounded by the known hyperplanes in general case. Note that in the entire procedure, only the measured FRFs of the baseline structure are required.

Furthermore, structural weights and/or stiffness can be minimized with respect to redundant parameters ($c_1, c_2, \ldots, c_s$) defined in the resulting feasible region if necessary. This minimization requires solving a linear-constrained non-linear-optimization problem in aids of some of non-linear programming techniques since the resulting mass and stiffness in equations (12) and (13) are non-linear functions of the redundant parameters ($c_1, c_2, \ldots, c_s$).

7. EXAMPLES

The proposed method is applied to a plate structure shown in Figure 3 by experiments. The example structure is a simply supported steel square plate having dimensions $800\,\text{mm} \times 800\,\text{mm} \times 3\,\text{mm}$. To account more practical situation, an uncertain boundary condition is given on purpose: the lower-left corner of the plate is supported by a linear spring having unknown stiffness. The measured natural frequencies and damping ratios of the plate are listed in Table 1. Two examples will be shown in this section. The first example, the simplest and straightforward case, is aimed to find an exact single structural modification only for a natural frequency reallocation of the plate. In the second one, more complicated case, both of the natural frequency and the modeshape are modified

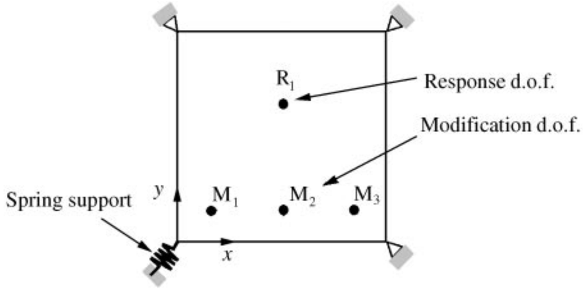

Figure 3. Modification d.o.f. (M_1, M_2 and M_3) and a response d.o.f. (R_1) on the example plate supported by three rigid supports and a spring support having unknown stiffness.

TABLE 1

Measured natural frequencies and damping ratios of an example plate

Mode no.	Natural frequency (Hz)	Damping ratio (%)
1	7·8	0·8
2	15·7	0·6
3	15·8	0·6
4	21·6	0·1
5	35·2	0·9
6	47·3	0·2

simultaneously by the multiple structural modifications through the approximate solution procedure described in section 6.

The objective of the first example is to find exact lumped mass–damper or mass–stiffness modification at node M_2 ($N_M = 1$) shown in Figure 3 which reallocates the second natural frequency from 15·7 to 18·0 Hz without any constraint on its modeshape ($N_R = 0$). In this case, an unique exact solution exists for the given natural frequency requirement as described in section 5. The measured point receptance of the baseline plate at node M_2 is

$$h^b_{M_2M_2}\,(18{\cdot}0\ \text{Hz}) = [-36{\cdot}9 + 1{\cdot}1\text{i}] \times 10^6. \tag{32}$$

In this case, the modal force **f** is scalar. The dynamic stiffness of the modification structure at node M_2 can be obtained from equations (11) and (32) as

$$d(18{\cdot}0\ \text{Hz}) = \frac{1}{h^b_{M_2M_2}(18{\cdot}0\ Hz)} = [27{\cdot}1 + 0{\cdot}8\text{i}] \times 10^3. \tag{33}$$

Since the real part of the dynamic stiffness d(18.0 Hz) is positive, stiffness element is determined to be added to node M_2 according to equation (13). Finally, the exact stiffness and damping parameters of the stiffness–damper modification for this natural frequency reallocation are found from equations (13) and (14) as

$$k = 27{\cdot}1\ \text{kN/m} \quad \text{and} \quad c = 7{\cdot}1\ \text{N s/m}. \tag{34}$$

Figure 4 shows the FRF change due to the resulting stiffness–damper modification. As one can see, the stiffness–damper modification given in equation (34) reallocates the second natural frequency to 18·0 Hz. Experimentally measured FRFs of the baseline structure can be used directly to form the modal force equation bypassing the numerical modelling process as shown in equation (4).

To show a more complicated application of the proposed method, the assignment of modeshape as well as that of natural frequency of the second mode is considered in the second example. Also extra constraints on the structural parameters are introduced. The objective of the second example is to find the structural elements added to three designated nodes M_1, M_2 and M_3 ($N_M = 3$) shown in Figure 3 which reallocate the second natural frequency from 15·7 to 18·0 Hz and place its nodal point to node R_1 ($\phi_n = 0$, $N_R = 1$) simultaneously. This nodal point assignment is aimed to minimize the vibration response at

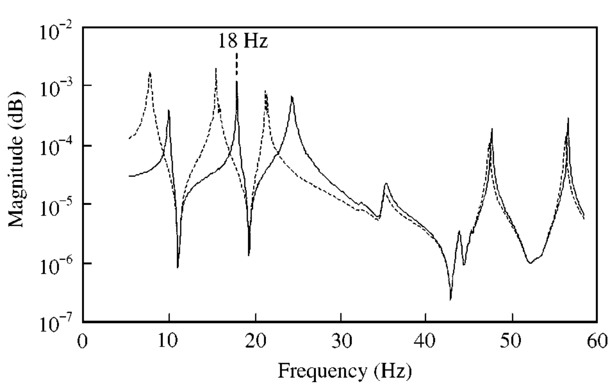

Figure 4. FRF change due to a stiffness–damper modification at node M_2 ($k = 27{\cdot}1$ kN/m, $c = 7{\cdot}1$ N s/m): - - - - -, original FRF of the plate; ——, modified FRF of the plate.

node R_1 caused by the excitation of the second mode. It is assumed that the structural modifications at the three nodes are restricted to be stiffness modifications only. The amounts of the stiffnesses are also assumed to be restricted up to 30·0 kN/m such that

$$k_j \leqslant \mathrm{K}_{max} = 30{\cdot}0\ \mathrm{kN/m} \quad \text{for } j = 1, 2, 3. \tag{35}$$

In this case, $\mathbf{H}^b_{RM}$ (18·0 Hz) is a 1×3 matrix and the modal force vector defined in equation (8) is underdetermined, hence infinite many exact structural modifications exist. The number of redundant parameters is 2 ($s = N_M - N_R = 2$). Instead of an exact solution, an approximated solution will be found through the solution procedure described in section 6 and the results were compared to the exact solution. To get the force response equation, i.e., equation (8), the cross receptances of the baseline plate between three modification nodes (M_1, M_2 and M_3) and one response node (R_1), i.e., $\mathbf{H}^b_{RM}$ (18·0 Hz) were measured as

$$\mathbf{H}^b_{RM}\,(18{\cdot}0\ \mathrm{Hz}) = [20{\cdot}9 - 1{\cdot}0\mathrm{i} \quad 30{\cdot}9 - 1{\cdot}8\mathrm{i} \quad 10{\cdot}6 - 0{\cdot}6\mathrm{i}] \times 10^{-6}. \tag{36}$$

The point and cross receptances between the three modification nodes, i.e., $\mathbf{H}^b_{MM}$ (18·0 Hz) were also measured to get the modal force equation, i.e., equations (4) as follows:

$$\mathbf{H}^b_{MM}\,(18{\cdot}0\ \mathrm{Hz}) = \begin{bmatrix} -66{\cdot}8 + 3{\cdot}6\mathrm{i} & -47{\cdot}9 + 2{\cdot}8\mathrm{i} & -4{\cdot}9 + 0{\cdot}5\mathrm{i} \\ & -36{\cdot}9 + 1{\cdot}1\mathrm{i} & -46{\cdot}2 + 3{\cdot}7\mathrm{i} \\ \text{sym.} & & -39{\cdot}0 + 2{\cdot}9\mathrm{i} \end{bmatrix} \times 10^{-6}. \tag{37}$$

Since the modal dampings of the plate shown in Table 1 are sufficiently small, the plate can be assumed to be an undamped system. Under the assumption that the plate is undamped, the real parts of the measured FRFs in equation (36) and (37) are used in the solution procedure while the imaginary parts are neglected, which have relatively small values compared to the real parts except in the vicinities of resonant frequencies. By using this assumption, all of the functions and variables considered in the second example become real-valued. From equation (16), underdetermined force vector $\mathbf{f}(\mathbf{c})$ (3×1) can be identified as

$$\mathbf{f}(\mathbf{c}) = [f_1(\mathbf{c}), f_2(\mathbf{c}), f_3(\mathbf{c})]^{\mathrm{T}} = c_1\mathbf{f}^1 + c_2\mathbf{f}^2, \tag{38}$$

where $\mathbf{c} = [c_1, c_2]^{\mathrm{T}}$ and c_1, c_2 are redundant parameters. In this case, $\mathbf{f}^0 = \mathbf{0}$ since $\phi_n = 0$ as shown in equation (16). Null vectors of $\mathbf{H}^b_{RM}$ (18·0 Hz) are $\mathbf{f}^1 = [-84{\cdot}2, 51{\cdot}0, 17{\cdot}5]^{\mathrm{T}} \times 10^{-2}$ and $\mathbf{f}^2 = [0, -32{\cdot}5, 94{\cdot}6]^{\mathrm{T}} \times 10^{-2}$. By substituting equation (38) into equation (19), $\mathbf{g}(\mathbf{c})$ can be obtained as

$$\mathbf{g}(\mathbf{c}) = [g_1(\mathbf{c}), g_2(\mathbf{c}), g_3(\mathbf{c})]^{\mathrm{T}} = c_1\mathbf{g}^1 + c_2\mathbf{g}^2, \tag{39}$$

where $\mathbf{g}^1 = [-31{\cdot}0, -13{\cdot}5, 26{\cdot}2]^{\mathrm{T}} \times 10^{-6}$ and $\mathbf{g}^2 = [-10{\cdot}9, 31{\cdot}7, 21{\cdot}9]^{\mathrm{T}} \times 10^{-6}$. From equation (19), the dynamic stiffnesses of the three modification structures can be written with respect to the redundant parameters c_1 and c_2 by using the calculated $\mathbf{f}(\mathbf{c})$ and $\mathbf{g}(\mathbf{c})$ as

$$d_j(18{\cdot}0\ \mathrm{Hz}) = \frac{f_j(\mathbf{c})}{g_j(\mathbf{c})} = \frac{c_1 f_j^1 + c_2 f_j^2}{c_1 g_j^1 + c_2 g_j^2} \quad \text{for } j = 1, 2, 3. \tag{40}$$

Hyperplanes $f_j(\mathbf{c}) = 0$ and $g_j(\mathbf{c}) = 0$ (for $j = 1, 2, 3$) in this example are plotted on c_1–c_2 plane as shown in Figure 5. The hyperplanes are lines in this case. Sub-regions A–F divided by these lines indicate the corresponding combinations of the three necessary structural modifications for achieving the given eigenproperties, which are determined from equations (20)–(23). Figure 5 reveals that only the sub-sets of all possible combinations of the

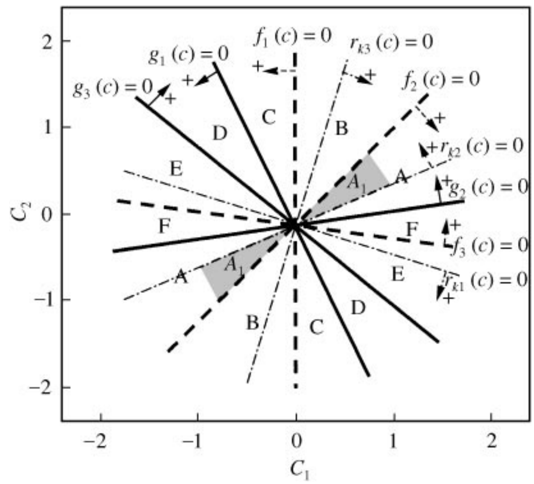

Figure 5. The relation between redundant parameters (c_1, c_2) and the feasible structural modifications at the three modification d.o.f. A (stiffness, stiffness, stiffness); B, D and F (stiffness, mass, stiffness); C (mass, mass, stiffness); E (stiffness, mass, mass). The region A_1 is feasible for the three stiffness modifications together with the constraints described in equation (35).

structural modifications are feasible in this case: these are (stiffness, stiffness, stiffness) modifications for region A, (stiffness, mass, stiffness) modifications for regions B, D and F, (mass, mass, stiffness) modifications for region C, and (stiffness, mass, mass) modifications for region E. These four combinations of structural modifications can be realized selectively by choosing the redundant parameters (c_1, c_2) in one of regions A–E. In order to obtain stiffness modifications at all three nodes, the redundant parameters (c_1, c_2) should be selected in region A. Extra constraints on the three stiffness defined in equation (31) can be written with respect to redundant parameters (c_1, c_2) from equations (27) as

$$r_{k1}(\mathbf{c}) = -\,8{\cdot}7c_1 - 3{\cdot}3c_2 \begin{cases} \geqslant 0 & \text{when } g_1(\mathbf{c}) > 0, \\ \leqslant 0 & \text{when } g_1(\mathbf{c}) < 0, \end{cases} \tag{41}$$

$$r_{k2}(\mathbf{c}) = -\,9{\cdot}1c_1 + 12{\cdot}8c_2 \begin{cases} \geqslant 0 & \text{when } g_2(\mathbf{c}) > 0, \\ \leqslant 0 & \text{when } g_2(\mathbf{c}) < 0, \end{cases} \tag{42}$$

$$r_{k3}(\mathbf{c}) = 6{\cdot}1c_1 - 2{\cdot}9c_2 \begin{cases} \geqslant 0 & \text{when } g_3(\mathbf{c}) > 0, \\ \leqslant 0 & \text{when } g_3(\mathbf{c}) < 0. \end{cases} \tag{43}$$

The feasible region of (c_1, c_2) for the stiffness modifications together with their constraints is obviously the intersection of region A and the constraint region defined in equations (41)–(43): that is region A_1 which can be written explicitly as

$$A_1 = \{(c_1, c_2) | 51{\cdot}0c_1 - 32{\cdot}5c_2 \geqslant 0 \text{ and } -9{\cdot}1c_1 + 12{\cdot}8c_2 \geqslant 0\}. \tag{44}$$

The feasible region A_1 is not empty. It reveals that the trial stiffness modifications for achieving the given eigenproperties together with their constraints in equation (35) are practically achievable in this case. Consequently, we can write down the stiffnesses at the three nodes explicitly from equations (13), (40) and (44) as follows:

$$k_1 = \frac{84{\cdot}2c_1}{31{\cdot}0c_1 + 10{\cdot}9c_2} \times 10^4 \text{ N/m}, \tag{45}$$

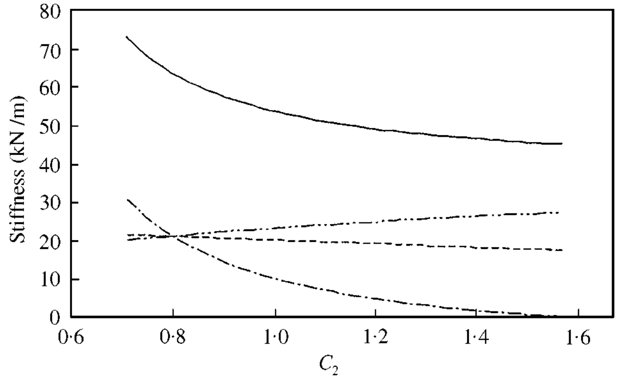

Figure 6. Variations of stiffness versus c_2 when $c_1 = 1$. Redundant parameters c_1 and c_2 belong to the feasible region A_1 in Figure 5. The stiffnesses are calculated from equations (45)–(47): ----, k_1; –·–·–, k_2; –··–, k_3; ——, total stiffness.

$$k_2 = \frac{51{\cdot}0c_1 - 32{\cdot}5c_2}{-13{\cdot}5c_1 + 31{\cdot}7c_2} \times 10^4 \text{ N/m}, \tag{46}$$

$$k_3 = \frac{17{\cdot}5c_1 + 94{\cdot}6c_2}{26{\cdot}2c_1 + 21{\cdot}9c_2} \times 10^4 \text{ N/m}, \tag{47}$$

where the redundant parameters (c_1, c_2), are defined in the region A_1.

Minimum modifications were found as the redundant parameters (c_1, c_2) vary in the feasible region A_1. Without loss of accuracy in this case, the minimum total stiffness was found as c_2 varies on the line $c_1 = 1$. Figure 6 shows the line search result. The minimum total stiffness of 44.9 kN/m was obtained when $c_1 = 1$ and $c_2 = 1{\cdot}57$. Three resulting stiffnesses are

$$k_1 = 17{\cdot}5,\ k_2 = 0{\cdot}0 \quad \text{and} \quad k_3 = 27{\cdot}4 \text{ kN/m}. \tag{48}$$

It is interesting that k_2 is determined to zero since the point $(c_1, c_2) = (1, 1{\cdot}57)$ is placed on the line $f_2(\mathbf{c}) = 0$ as shown in Figure 5. Figure 7 and 8 show that the second mode of the modified plate has natural frequency of 18·0 Hz and nodal point at node R_1 by the additions of calculated stiffnesses.

The resulting stiffnesses in equation (48) were calculated under the assumption that the plate is undamped. To examine the validity of this assumption, the approximated stiffnesses in equation (48) were compared to an exact solutions which are calculated from the same FRFs in equations (36) and (37) without neglecting the imaginary parts of those FRFs. To find the exact modifications, complex-valued $\mathbf{f}(\mathbf{c})$ and $\mathbf{g}(\mathbf{c})$ were calculated from the measured FRFs in equations (36) and (37), and the same redundant parameters $(c_1, c_2) = 1$, 1·57) were used. Then the complex-valued dynamic stiffnesses d_j (18·0 Hz) (for $j = 1, 2, 3$) in equation (40) were obtained as

$$d_1\ (18{\cdot}0 \text{ Hz}) = (17{\cdot}5 + 0{\cdot}9\text{i}) \times 10^3, \tag{49}$$

$$d_2\ (18{\cdot}0 \text{ Hz}) = (0{\cdot}0 + 0{\cdot}1\text{i}) \times 10^3, \tag{50}$$

$$d_3\ (18{\cdot}0 \text{ Hz}) = (27{\cdot}2 + 1{\cdot}9\text{i}) \times 10^3. \tag{51}$$

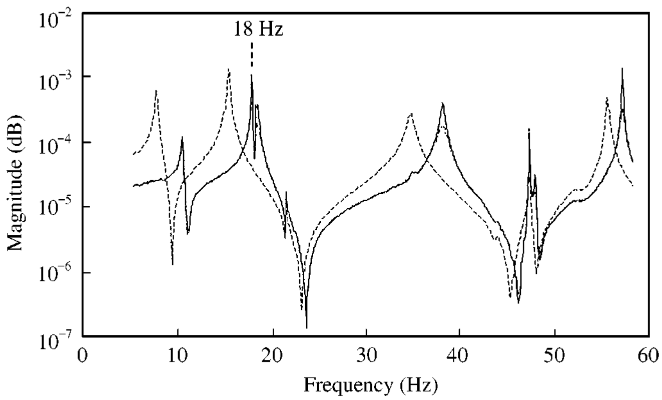

Figure 7. FRF changes due to structural modifications: - - - -, original FRF of the plate; —, modified FRF of the plate after the approximated stiffness modifications in equation (48); - · · · -, modified FRF of the plate after the exact stiffness–damper modifications in equations (52) and (53).

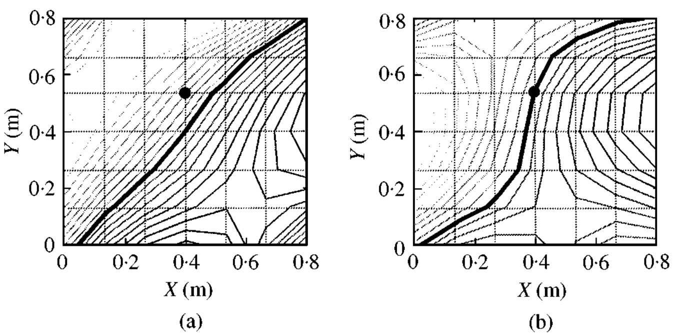

Figure 8. Contour plots of the modeshapes of the plate before and after the stiffness modifications in equation (48), $k_1 = 17{\cdot}5$, $k_2 = 0{\cdot}0$ and $k_3 = 27{\cdot}4$ kN/m: ▬, nodal line; ●, desired nodal point; (a) original modeshape of the second mode of the plate (15·5 Hz); (b) modified modeshape after the stiffness modifications (18·0 Hz).

From equations (13) and (14), the corresponding exact structural parameters of the stiffness–damper modifications were obtained as

$$k_1 = 17{\cdot}5, \quad k_2 = 0{\cdot}0 \quad \text{and} \quad k_3 = 27{\cdot}2\ \text{kN/m}, \tag{52}$$

$$c_1 = 8{\cdot}0, \quad c_2 = 0{\cdot}9 \quad \text{and} \quad c_3 = 16{\cdot}8\ \text{Ns/m}. \tag{53}$$

Comparing equations (48) and (52), the approximated stiffnesses in equation (48) differ from the exact solutions up to 0·8%. However, the exact damping modifications in equation (53) are needed to achieve the imaginary parts of the complex dynamic stiffnesses in equations (49)–(51). Figure 7 shows that the imaginary parts of the complex dynamic stiffnesses in equations (49)–(51). Figure 7 shows that these additional damping modifications reduce the frequency response of the plate in the vicinities of the modified natural frequencies. But these damping additions do not affect the system natural frequencies considerably. The approximated stiffness modifications in equation (48) and the exact stiffness–damper modifications in equations (52) and (53) yield the same natural frequency of 18·0 Hz: the natural frequency difference is observed to be less than the frequency resolution used in this experiment, i.e., 0·08 Hz. This indicates that the assumption used in calculating the approximated stiffnesses is valid in this low-damping case. However, if the damping of the baseline structure is not negligible, the approximated modification will produce large errors of resulting eigen properties from those obtained from exact solutions. In this case, only the exact structural modifications are valid, and the simple vector space approach described in section 6 cannot be applied.

It is interesting that the unknown stiffness support was left to unknown value in calculating the exact structural modifications. Since the proposed method is based on the experimental data which reflect the effect of the uncertain boundary condition, extra efforts to identify the uncertainty is not needed. This point shows an advantage of the proposed experimental method when it is applied to complex real structures which normally require expensive numerical modelling and verification process.

8. CONCLUSIONS

An analytical approach for the structural modification using multiple lumped masses, dampers and stiffnesses was presented to exactly achieve the pre-determined system natural frequency and modeshape simultaneously. An FRF-based substructure-coupling concept is used for the identification of structural parameters. In the solution procedure, only the measured FRFs at the designated positions are required without any need of the numerical model of an existing structure.

When the number of modeshape constraints and that of structural modification are equal, a unique exact structural modification exist and the modification can be identified straightforwardly. When infinite many exact modifications exist, the modification consists of the summation of redundant modifications. The redundant modifications can be used to meet the hardware restrictions on the structural modifications. Under the assumption that the existing structure is undamped, this paper suggests a vector space approach to examine the feasibility of the potential structural modifications among the infinite many modifications. Though the approach is not straightforward, it can provide the explicit expressions of the feasible structural modifications.

In the example of a plate structure, minimum stiffness modification were identified efficiently to reallocate a natural frequency and a nodal point. For damped systems, not only mass and stiffness but also damping modification is required to exactly get the desired modes. However, the result of the example reveals that the imaginary parts of the measured FRFs are related especially to the resulting damping modification, which does not affect the system modes considerably in lightly damped systems. Hence, the resulting approximated modifications under the undamped-system assumption are found to be valid for lightly damped systems.

The modal change, which is considered in this paper, can be useful to modify the other system dynamic behaviors. In the example of the paper, to show one of this usefulness, the nodal point assignment is considered to minimize the vibration response at a specific position. However, the improvement of the vibration at one position can make it worse at the other positions. Meanwhile, modifying too many vibration responses may require impractical structural modifications. Hence, in order to get the efficient modifications, the target modes should be determined carefully according to the desired dynamic characteristics before conducting the structural modifications.

The identified structural modifications of the proposed method are exact when the measured FRFs are free of noise. But sometimes it is difficult to get accurate FRFs. Further works should deal with the effects of the measurement errors on resulting modifications to obtain a reliable structural modification.

REFERENCES

1. Q. Zhang, R. J. Allemang and D. L. Brown April 1989 *Journal of Analytical and Experimental Modal Analysis* **4**, 39–44. Prediction of mass modification for desired natural frequencies.
2. R. J. Pomazal and V. W. Snyder 1971 *AIAA Journal* **9**, 2216–2221. Local modifications of damped linear systems.
3. J. O. Halliquist 1976 *Journal of Sound and Vibration* **44**, 449–459. An efficient method for determining the effect of mass modifications in damped systems.
4. W. Wang, Q. Zhang, R. J. Allemang and D. L. Brown 1990 *Proceedings of the 8th International Modal Analysis Conference*, 946–953. Optimization of structural redesign with dynamic constraints.
5. J. F. Baldwin and S. G. Hutton 1985 *American Institute of Aeronautics and Astronautics Journal* **23**, 1737–1743. Natural modes of modified structure.
6. Y. M. Ram, S. G. Braun and J. Blech 1988 *Journal of Sound and Vibration* **125**, 203–209. Structural modifications in truncated systems by the Rayleigh-Ritz method.
7. P. Avitabile and J. C. O'Callahan 1991 *The International Journal of Analytical and Experimental Modal Analysis* **6**, 215–235. Understanding structural dynamic modification and the effects of truncation.
8. I. Bucher and S. Braun 1993 *Mechanical Systems and Signal Processing* **7**, 217–283. The structural modification inverse problem: an exact solution.
9. E. K. Yee and Y. G. Tsuei 1989 *American Institute of Aeronautics and Astronautics Journal* **27**, 1083–1088. Direct component modal synthesis technique for system dynamic analysis.
10. E. K. L. Yee and Y. G. Tsuei 1989 *ASME Transactions on Journal of Dynamic Systems Measurement and Control* **111**, 403–408. A method for modifying dynamic properties of undamped mechanical systems.
11. T. Li and J. He 1997 *Proceedings of the International Modal Analysis Conference*, 1270–1276. Optimization of dynamic characteristics of a mdof systems by mass and stiffness modification.
12. Y.-H. Park and Y.-s. Park 2000 *Journal of Sound and Vibration* **229**, 1235–1255. Structure optimization to enhance its natural frequencies based on measured frequency response functions.
13. B. Noble ad J. W. Daniel 1988 *Applied Linear Algebra. Englewood Cliffs, NJ*: Prentice-Hall, second edition.